Comparison of Integrated Digital Radiometer with Concurrent Water Vapor Radiometer using the Alphasat Receivers in Milan, Italy

Michael Zemba[1], James Nessel[1], Lorenzo Luini[2], Carlo Riva[2]
[1] NASA Glenn Research Center: Advanced High Frequency Branch, Cleveland, OH, USA
[2] Politecnico di Milano: Dipartimento di Elettronica, Informazione e Bioingegneria, Milan, Italy

***Abstract*— In June 2014, NASA Glenn Research Center (GRC) and the Politecnico di Milano (POLIMI) jointly deployed a pair of coherent 20 GHz and 40 GHz beacon receivers to the POLIMI campus in Milan, Italy to characterize the atmospheric channel at Ka- and Q-band within the framework of the Alphasat experiment. The Milan receivers observe the continuous-wave beacons broadcast over Europe by the Aldo Paraboni Technology Demonstration Payload (TDP #5), and, in September 2017, both channels were upgraded to incorporate a novel digital radiometer (DR) measurement which NASA has recently employed in other propagation measurement campaigns. In November 2016, a co-located water vapor radiometer (WVR) was also installed at POLIMI, and the concurrent data from both the WVR and DR thusly enables validation of this new DR technique against the established WVR. Herein, we preliminarily investigate the calibration of the DR measurements using the WVR data and also assess a calibration method that may be implemented where WVR data is not readily available.**

Index Terms—*Alphasat, Aldo Paraboni TDP #5, radiowave propagation, propagation losses, radiometry.*

I. Introduction

NASA's participation in the Alphasat propagation campaign began with the installation of coherent Ka- and Q-band receivers at POLIMI in 2014 [1] and has since grown through the deployment of Q-band receivers to Heriot-Watt University in Edinburgh, Scotland (March 2016, [2]) and the Madrid Deep Space Communications Complex in Robledo de Chavela, Spain (March 2017, [3]). During the development of the Scotland terminal, a novel digital radiometric procedure was conceived and implemented wherein the sky brightness, T_{sky}, can be approximated by integrating the noise power in the band around the signal, excluding the power of the beacon itself. The ultimate objective of this procedure is to derive a satisfactory estimate of the clear-sky attenuation which can then be used to calibrate the total attenuation of the beacon measurement. Such a measurement, integrated directly into the beacon receiver at low cost, has the potential to greatly simplify calibration of beacon measurements in contrast to the current methods of deriving the clear-sky attenuation through either supplementary radiometer measurements or numerical weather prediction models. However, to reliably implement this digital radiometer (DR) technique first requires accurate calibration of the integrated noise power to a corresponding sky brightness temperature.

The installation of a Radiometer Physics GmbH (RPG) water-vapor radiometer (WVR) at the POLIMI campus in

Fig. 1. Photographs of the Ka/Q-band beacon receivers (top), Radiometer Physics GmbH water vapor radiometer (middle) and an overhead view (bottom) of the receiver location at the POLIMI campus in Milan, Italy.

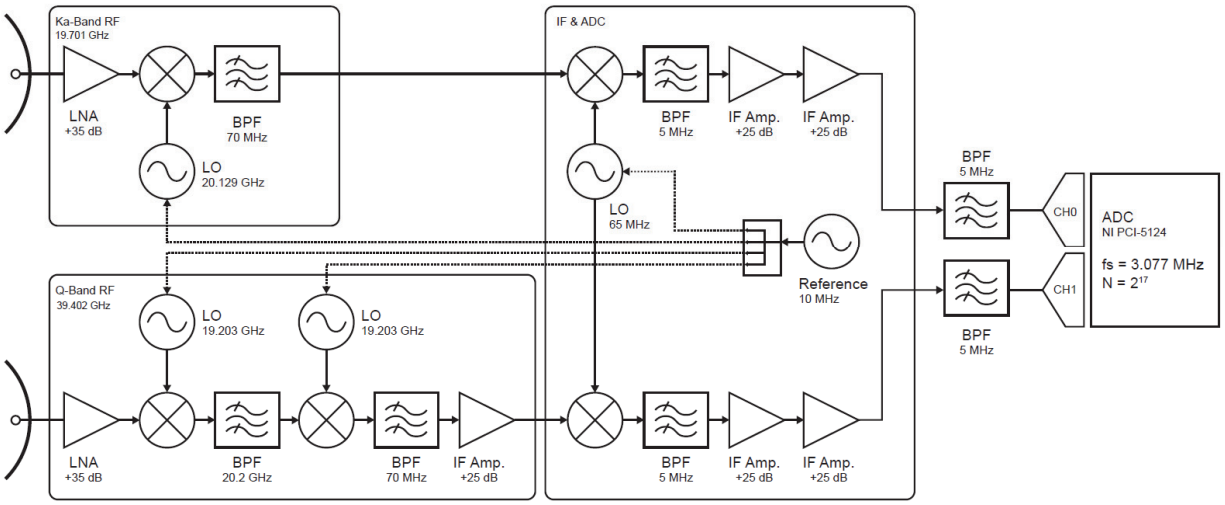

Fig. 2. Block diagram of the Milan beacon receiver design, which was upgraded in September 2017 to a final IF of 5 MHz and a wider IF bandwidth of 1 MHz to enable implementation of the digital radiometer measurement within the receiver software.

November 2016 provided a unique opportunity to validate these digital noise power measurements with the co-located WVR data, and, to this end, the Milan hardware was upgraded in September 2017 to enable the DR measurements akin to the Scotland and Madrid designs. These modifications consisted of adjusting the final downconverted frequency from 455 kHz to 5 MHz as well as widening the final system bandwidth to 1 MHz to allow for approximately 1 MHz over which to integrate the noise power. These concurrent DR and WVR measurements have been operational since October 2017, and this paper preliminarily investigates the use of this data to calibrate the digital measurements using the RPG radiometer. Furthermore, we also compare a calibration method for the DR that is implemented without use of WVR data and compare the results to the WVR calibration to infer its accuracy.

II. Experiment Design

A. Ka-/Q-band Beacon Receivers

The design of the Ka and Q-band beacon receivers is presented in the block diagram of Fig. 2. The Ka-band and Q-band channels utilize 1.2m and 0.6m Cassegrain reflectors, respectively. Both antennas have a gain of 45.6 dBi and beamwidth of 0.9° -- this narrow beamwidth, combined with the inclined orbit of Alphasat (3° maximum inclination), requires tracking of the satellite. This is implemented through electronic positioners that update the antenna pointing once per minute with a resolution of 0.01° in both azimuth and elevation utilizing Alphasat's Orbital Ephemeris Message (OEM) data.

Each channel is downconverted at the antenna feed from the beacon frequencies (19.701 GHz and 39.402 GHz) to an IF of 70 MHz inside thermally controlled enclosures that keep the electronics stable within ±0.01°C (cold plate temperature) or ±2°C (air temperature). In addition, the LNAs for each channel are equipped with supplementary temperature control that maintains LNA temperature within ±0.1°C. All local oscillators are referenced to a common ultra-stable 10 MHz citrine oscillator. After downconversion, the 70 MHz signals from each channel are run to a common IF enclosure (also temperature controlled ±1.0°C) where one more downconversion occurs to the final IF of 5 MHz before the signal is run over coaxial cable to the digitizer and data acquisition system.

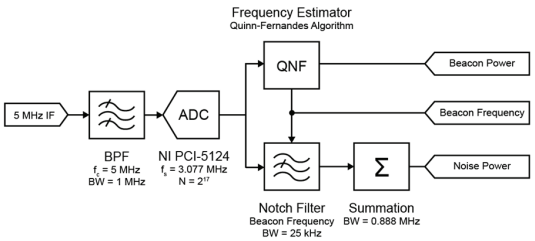

Fig. 3. Block diagram of the digital signal processing steps used to derive the beacon power, frequency, and integrated noise power after digitization of the 5 MHz signal.

B. Integrated Digital Radiometer

The signal processing after digitization is represented in the block diagram of Fig. 3: the downconverted 5 MHz beacon signal, having been filtered with a bandwidth of 1 MHz prior to digitization, is bandpass sampled at $f_s = 3.077$ MHz with $N = 2^{17}$ samples. The digitized spectrum is then supplied to two separate algorithms that calculate the beacon power and the noise power. A modified version of the Quinn-Fernandes frequency estimator [4] is used to estimate the peak frequency and power of the beacon with greatly improved accuracy over a simple FFT peak search, as described in [5]. The beacon frequency calculated by this algorithm is then used as the center of a notch filter of 25 kHz bandwidth, applied to the digitized spectrum to remove the beacon signal. After applying the notch, the noise power is integrated over a bandwidth of 0.888 MHz to capture the

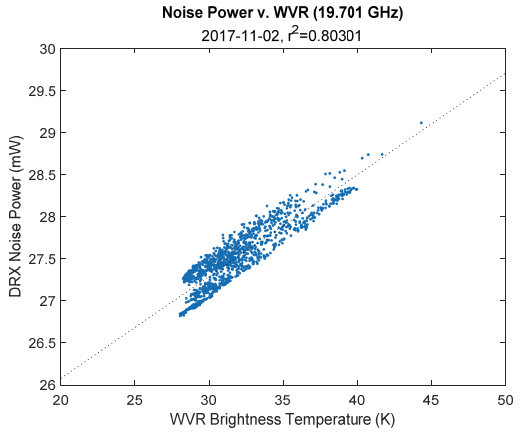

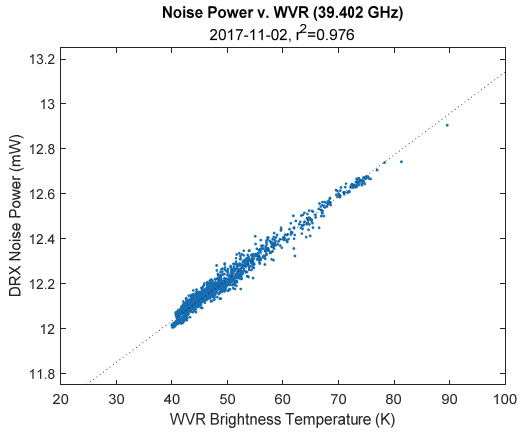

Fig. 4. Scatter plots of the digital radiometer noise power and water vapor radiometer brightness temperature for the Ka (top) and Q (bottom) channels with linear regressions of each.

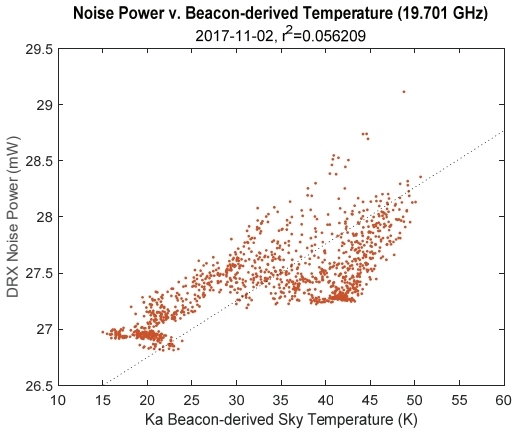

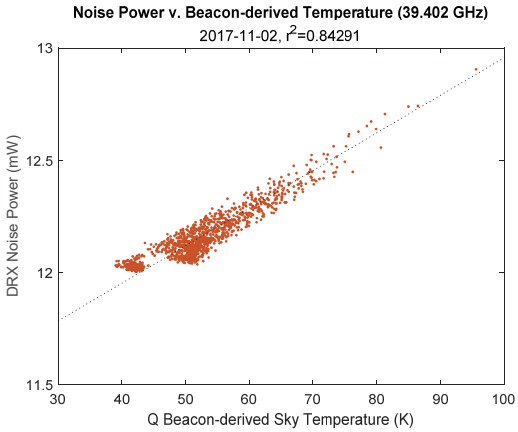

Fig. 5. Scatter plots of digital radiometer noise power and beacon-derived brightness temperature utilizing ECMWF data for the Ka (top) and Q (bottom) channels and associated linear regressions.

majority of the 1 MHz band while avoiding the transition regions of the filter. While a 1 MHz bandwidth is rather narrow as compared to a traditional radiometer measurement, the goal of this work is to demonstrate that reasonable radiometric measurements, for the purpose of deriving clear-sky calibration data, can be implemented alongside a standard beacon receiver system and function within the associated design constraints.

III. Data Analysis & Calibration

A. Calibration with Water Vapor Radiometer

Calibration of the noise power measurement using the WVR data is a straightforward process whereby a linear fit is applied to relate the DR noise power to the WVR sky brightness, treating the WVR-measured sky temperature as the true T_{sky}. For the purposes of this paper, a single characteristic low attenuation day was used as an example to demonstrate the methodology. For processing larger periods of data, care should be taken to remove high attenuation events which may skew the linear relationship between noise power and sky temperature. For example, one clear sky day per month could be used to derive calibration coefficients to apply for calibration of the rest of the month's noise power measurements, or to derive a singular clear-sky attenuation offset applied to the rest of the monthly beacon measurements. Fig. 4 presents scatter plots of the DR integrated noise power vs. WVR brightness temperature for the example day, 2017-11-02, on both the Ka (top) and Q (bottom) channels. Throughout this day, small attenuation events were regularly observed, but the beacon attenuation remained below 3 dB and WVR brightness remained below 100 K. A strong linear relationship was observed between the DR noise power and WVR temperature with a linear regression yielding coeffecients of 8.28 K/mW slope and -195.9 K offset for the Ka channel and 54.1 K/mW slope and -611.0 K offset for the Q channel with r^2 of 0.80 and 0.98, respectively. These coefficients were then applied to the DR noise power timeseries to translate the noise power measurement into a sky temperature.

B. Calibration with ECMWF

While the previous calibration provides an easy reference from noise power to brightness temperature where WVR data is available, an effort was also made to develop a calibration of comparable accuracy while avoiding the requirement of local

radiometer data. To calibrate the noise power measurement without an external reference (radiometer) or internal reference (noise diode), an independent assessment of the clear sky attenuation is necessary to determine the absolute attenuation due solely to atmospheric components such as absorption due to clouds and gases. This can be provided through the numerical weather prediction (NWP) models of the European Centre for Medium-Range Weather Forecasts (ECMWF). ECMWF results for Milan can be used to obtain estimates of total path attenuation and brightness temperature every 6 hours, which can be used to estimate the clear sky reference level. Once the beacon receiver data is referenced to this initial level, the beacon data is then transformed to an estimated sky brightness temperature via the radiative transfer equation and plotted against the digital radiometer noise power measurement. As in the WVR calibration, a linear fit is again applied to the data to extract the scaling coefficients. Fig. 5 shows the scatter plots of the DR noise power and beacon-derived brightness temperature for Ka-band (top) and Q-band (bottom). As could be expected, the linear relationship is not as strong as in the WVR calibration (Fig. 4), but this approach does allow for calibration of the noise power data without necessitating a co-located radiometer. The resulting coefficients from the fit to the beacon-derived temperature for this approach were 19.8 K/mW and -509 K for the Ka channel and 59.7 K/mW and -673.9 K for the Q channel. This approach has also been validated with a tip calibration and is further detailed in [6]. In addition, the Madrid Alphasat receiver has explored the use of an internal noise diode to perform calibration using an internal reference [3].

IV. Results

With the integrated noise power of the digital radiometer calibrated to a brightness temperature through both approaches (using the WVR and using the ECMWF), the timeseries of brightness temperature is plotted in Fig. 6 as compared to the measured brightness temperature of the WVR for both the 19.701 GHz and 39.402 GHz channels. While there is variability between each measurement, particularly in the DR as calibrated with the ECMWF, there is a reasonable agreement between each measurement for a majority of the observation period. Some diurnal variation was noted in the receiver beacon power and noise power (<1 dB), potentially due to small pointing error and/or variability in physical antenna temperature. While these small variations are normally not of concern when considering attenuation statistics over the 40 dB dynamic range of the system, they become much more noticeable when examining low attenuation events for calibration of the noise power. This diurnal variation is expected to have contributed to the error visible in Fig. 6, particularly in the DRX as calibrated with ECMWF where any error in beacon power is compounded with any error in noise power.

In addition, the calibrated sky brightness was translated into total attenuation, as shown in Fig. 7, where it can be compared to the attenuation measured directly with the beacon receivers. Here again it can be seen that some periods throughout the day show better agreement than others, but generally speaking both the DR-derived attenuation and WVR-derived attenuation match reasonably with the measured signal level.

To quantify accuracy of each calibration, the RMS error was assessed as plotted in Fig. 8. In terms of brightness temperature, the peak RMS error was 15.3 K when calibrated via ECMWF and 3.09 K when calibrated via the WVR. The total RMS error for the example period when using the WVR calibration was 1.3 K on the Ka channel and 1.2 K on the Q channel. For the ECMWF calibration, the total RMS error was 4.9 K (Ka) and 5.8 K (Q). In terms of attenuation, the peak RMS error for the observation period was 0.5 dB on the Q channel and 0.1 dB on the Ka channel, with comparable error between the WVR attenuation and ECMWF attenuation due to diurnal variation in measured beacon power. The total RMS error when deriving attenuation from the WVR data was 0.06 dB on the Ka channel and 0.15 dB on the Q channel. For the digital radiometer calibrated via ECMWF, the total RMS error in attenuation was 0.07 dB (Ka) and 0.15 dB (Q).

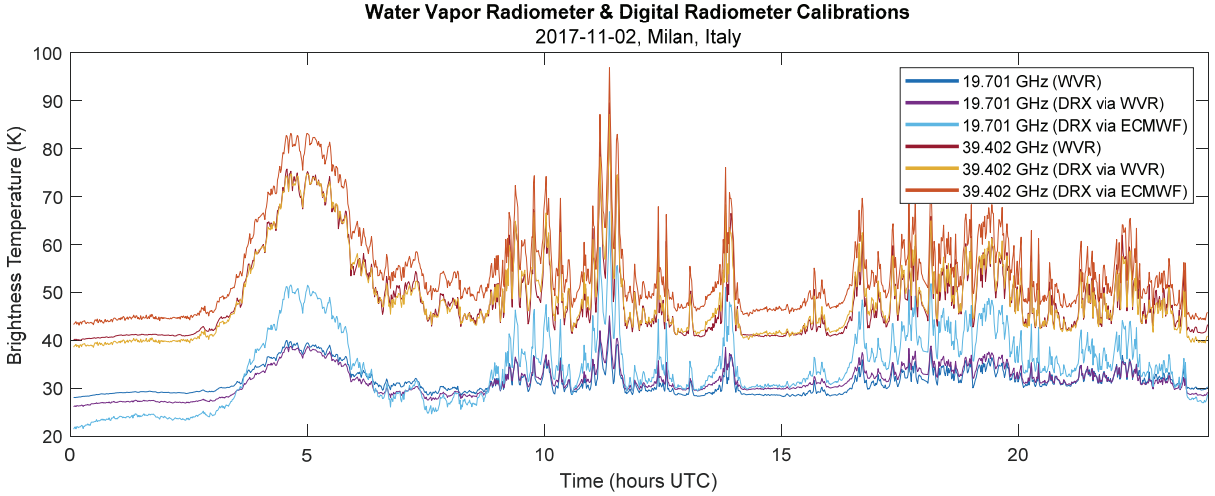

Fig. 6. Timeseries brightness temperature for an example day comparing the sky brightness temperature as measured directly with the water vapor radiometer, as derived from the digital radiometer when calibrated with the WVR, and as derived from the digital radiometer when calibrated with the ECMWF technique.

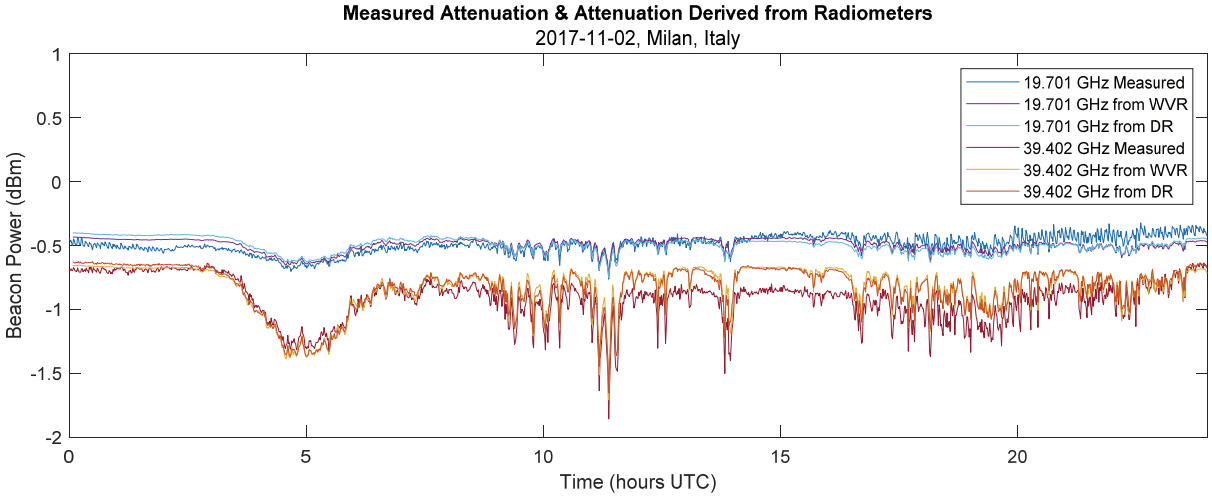

Fig. 7. Block diagram of the digital signal processing steps used to derive the beacon power, frequency, and integrated noise power after digitization.

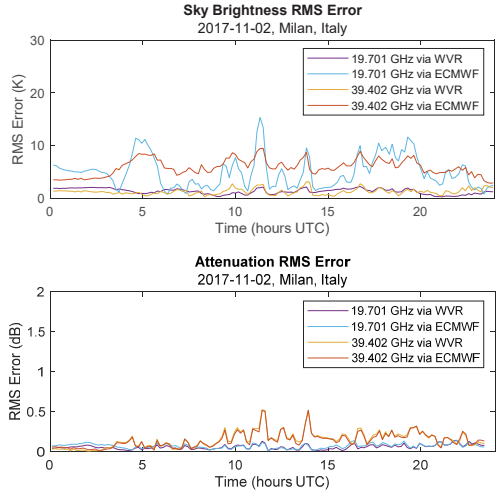

Fig. 8. The RMS error associated with each calibration method in terms of brightness temperature (top) and in terms of attenuation (bottom).

V. Conclusions

Herein, we have preliminarily demonstrated that errors less than 15.3 K of brightness temperature and less than 0.5 dB of attenuation can be achieved when integrating a digital radiometer within a beacon receiver system as detailed here. Several methods are available for calibration, and this work has demonstrated the use of a co-located water vapor radiometer for calibration as well as method that uses ECMWF data and avoids the requirement of additional instrumentation. While there remain refinements that can be made to the calibration processes, the currently demonstrated level or error is quite reasonable, particularly considering the negligible overhead associated with implementing the digital radiometer technique as deployed in the Alphasat receivers of Milan, Edinburgh, and Madrid. Future work will continue to refine these calibration procedures and investigate consistency of the calibrations over longer periods of time.

References

[1] M. Zemba, J. Nessel, L. Luini, C. Riva, “Three Years of Atmospheric Characterization at Ka/Q-band with the NASA/POLIMI Alphasat Receiver in Milan, Italy,” 12th European Conf. on Antennas and Propag., London, United Kingdom. April 9-13 2018.

[2] M. Zemba, J. Nessel, N. Sia, G. Goussetis, “Two Years of Atmospheric Measurements in Edinburgh, Scotland,” 22nd Ka and Broadband Communications Conference, Niagara Falls, Canada. October 15 – 18, 2018.

[3] M. Zemba, J. Nessel, D. Morabito, “Design of a Combined Beacon Receiver and Digital Radiometer for 40 GHz Propagation Measurements at the Madrid Deep Space Communications Complex,” 23rd Ka and Broadband Communications Conference, Trieste, Italy, October 2017.

[4] B.G. Quinn & J.M. Fernandes, “A Fast Technique for the Estimation of Frequency”, Biometrika, vol. 78, pp. 489–497, Sept. 1991.

[5] M. Zemba, J. Morse, J. Nessel, "Frequency Estimator Performance for a Software-Based Beacon Receiver," 2014 IEEE Int. Symp. on Antennas and Propag., Memphis, TN. July 6-11 2014.

[6] J. Nessel, G. Gousetis, M. Zemba, J. Houts, “Design and Preliminary Results from Edinburgh, UK Alphasat Q-band Propagation Terminal,” 22nd Ka and Broadband Communications Conf., Cleveland, OH, October 2016.

[7] A. Paraboni, A. Vernucci, L. Zuliani, E. Colzi, A. Martellucci, “A New Satellite Experiment in the Q/V band for the Verification of Fade Countermeasures Based on the Spatial Non-Uniformity of Attenuation,” 2nd European Conf. on Antennas and Propag., Edinburgh, UK. November, 2007.

[8] B. G. Quinn, "Estimating Frequency by Interpolation…," IEEE Trans. Sig. Proc., vol. 42, no. 5, May 1994.

[9] J. Nessel, J. Morse, M. Zemba, C. Riva, L. Luini, “Performance of the NASA Beacon Receiver for the Alphasat Aldo Paraboni TDP5 Propagation Experiment,” 2015 IEEE Aerospace Conference, p. 1- 8, Big Sky, Montana. March 7 – 14, 2015.